NASA/TP-1999-206574

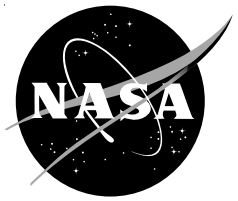

A Reassessment of Heavy-Duty Truck Aerodynamic Design Features and Priorities

Edwin J. Saltzman
Analytical Services & Materials
Edwards, California

Robert R. Meyer, Jr.
Dryden Flight Research Center
Edwards, California

June 1999

The NASA STI Program Office…in Profile

Since its founding, NASA has been dedicated to the advancement of aeronautics and space science. The NASA Scientific and Technical Information (STI) Program Office plays a key part in helping NASA maintain this important role.

The NASA STI Program Office is operated by Langley Research Center, the lead center for NASA's scientific and technical information. The NASA STI Program Office provides access to the NASA STI Database, the largest collection of aeronautical and space science STI in the world. The Program Office is also NASA's institutional mechanism for disseminating the results of its research and development activities. These results are published by NASA in the NASA STI Report Series, which includes the following report types:

- TECHNICAL PUBLICATION. Reports of completed research or a major significant phase of research that present the results of NASA programs and include extensive data or theoretical analysis. Includes compilations of significant scientific and technical data and information deemed to be of continuing reference value. NASA's counterpart of peer-reviewed formal professional papers but has less stringent limitations on manuscript length and extent of graphic presentations.

- TECHNICAL MEMORANDUM. Scientific and technical findings that are preliminary or of specialized interest, e.g., quick release reports, working papers, and bibliographies that contain minimal annotation. Does not contain extensive analysis.

- CONTRACTOR REPORT. Scientific and technical findings by NASA-sponsored contractors and grantees.

- CONFERENCE PUBLICATION. Collected papers from scientific and technical conferences, symposia, seminars, or other meetings sponsored or cosponsored by NASA.

- SPECIAL PUBLICATION. Scientific, technical, or historical information from NASA programs, projects, and mission, often concerned with subjects having substantial public interest.

- TECHNICAL TRANSLATION. English-language translations of foreign scientific and technical material pertinent to NASA's mission.

Specialized services that complement the STI Program Office's diverse offerings include creating custom thesauri, building customized databases, organizing and publishing research results…even providing videos.

For more information about the NASA STI Program Office, see the following:

- Access the NASA STI Program Home Page at ***http://www.sti.nasa.gov***

- E-mail your question via the Internet to help@sti.nasa.gov

- Fax your question to the NASA Access Help Desk at (301) 621-0134

- Telephone the NASA Access Help Desk at (301) 621-0390

- Write to:
  NASA Access Help Desk
  NASA Center for AeroSpace Information
  7121 Standard Drive
  Hanover, MD 21076-1320

NASA/TP-1999-206574

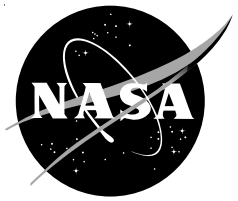

A Reassessment of Heavy-Duty Truck Aerodynamic Design Features and Priorities

Edwin J. Saltzman
Analytical Services & Materials
Edwards, California

Robert R. Meyer, Jr.
Dryden Flight Research Center
Edwards, California

National Aeronautics and
Space Administration

Dryden Flight Research Center
Edwards, California 93523-0273

June 1999

NOTICE

Use of trade names or names of manufacturers in this document does not constitute an official endorsement of such products or manufacturers, either expressed or implied, by the National Aeronautics and Space Administration.

Available from the following:

NASA Center for AeroSpace Information (CASI)
7121 Standard Drive
Hanover, MD 21076-1320
(301) 621-0390

National Technical Information Service (NTIS)
5285 Port Royal Road
Springfield, VA 22161-2171
(703) 487-4650

ABSTRACT

Between 1973 and 1982, the NASA Dryden Flight Research Center conducted "coast-down" tests demonstrating means for reducing the drag of trucks, buses, and motor homes. Numerous configurations were evaluated using a box-shaped test van, a two-axle truck, and a tractor-semitrailer combination. Results from three configurations of the test van are of interest now in view of a trucking industry goal of a 0.25 drag coefficient for tractor-semitrailer combinations. Two test van configurations with blunt-base geometry, similar to present day trucks (one configuration has square front corners and the other has rounded front corners), quantify the base drag increase associated with reduced forebody drag. Hoerner's equations predict this trend; however, test van results, reinforced by large-scale air vehicle data, indicate that Hoerner's formula greatly underestimates this dependence of base drag on forebody efficiency. The demonstrated increase in base drag associated with forebody refinement indicates that the goal of a 0.25 drag coefficient will not be achieved without also reducing afterbody drag. A third configuration of the test van had a truncated boattail to reduce afterbody drag and achieved a drag coefficient of 0.242. These results are included here and references are identified for other means of reducing afterbody drag.

NOMENCLATURE

A	conventional reference area, $h \times w$, ft^2
A'	NASA Dryden–designated reference area, $h' \times w$, ft^2
A_b	base area, ft^2, $A_b = A'$ for test van configurations A through F
A_c	maximum projected cross-sectional area, ft^2
A_w	wetted area of forebody, ft^2
c	base pressure profile factor, $c = 0.92$ for air vehicles and $c = 0.95$ for test van*
C_D	total aerodynamic drag coefficient, $C_{D_{f,b}} + C_{D_b}$, reference area = A' for test van
C_{D_A}	drag coefficient of test van configuration A (all square corners)
C_{D_b}	base drag coefficient, reference area A_b, $C_{D_b} = c \cdot \lvert -C_{P_b} \rvert$
C_{D_f}	forebody drag coefficient,† $C_D - C_{D_b}$
$C_{D_{f,b}}$	forebody drag coefficient, reference A_b
$C_{D_{f,w}}$	forebody drag coefficient, reference A_w
C_{F_e}'	equivalent skin friction coefficient of forebody, $C_{F_e}' = C_{D_{f,w}}$
COE	cab over engine

*The profile factor for ground vehicles is assumed to be closer to unity than for air vehicles because base flow separation line (station) for ground vehicles is relatively less complex and free of upstream leakage.

†C_{D_f} can have two different reference areas, either $C_{D_{f,b}}$ or $C_{D_{f,w}}$.

C_{P_b}	base pressure coefficient, $(P_b - P_\infty)/\bar{q}$
d_{eff}	effective diameter of the vehicle, $d_{eff} = \sqrt{\frac{4A_c}{\pi}}$, ft
DOT	Department of Transportation
h	height of vehicle from ground to top surface, ft or in.
h'	height of cargo container part of vehicle, ft or in.
K	numerator coefficient for Hoerner's equation
l	length of vehicle, ft or in.
P_b	base pressure, lb/ft^2
P_∞	ambient pressure, lb/ft^2
$\bar{q}$	dynamic pressure, lb/ft^2, $1/2\rho V^2$
r	radius of rounded front corners, in.
V	velocity of test van in calm wind conditions, mi/hr or ft/sec
w	width of cargo container part of vehicle, ft or in.
ΔC_D	reduction in drag coefficient of a test van configuration relative to C_{D_A}
ρ	ambient density of air, slug/ft^3

INTRODUCTION

The NASA Dryden Flight Research Center (Edwards, California) became involved with ground vehicle aerodynamics during the "oil crisis" of the early 1970's. At that time, most designers of motor homes, buses, and heavy-duty trucks ignored aerodynamic considerations when determining vehicle shape. Primary emphasis was given to ease of fabrication and avoiding rounded corners that would diminish inside volume. The resulting configurations were box-like and represented great opportunity for aerodynamic refinement.

At NASA Dryden,* experimental effort emphasized real vehicles rather than subscale models. At the onset of the "energy crisis," potential existed for demonstrating significant improvements in drag reduction by applying the simple "coast-down" (deceleration) techniques to ground vehicles that had been used by earlier experimenters.[1–3] Experimenters at NASA Dryden had confidence in the coast-down method because it is analogous to the accelerometer method of measuring aircraft drag for "coasting," or "power off," flight.[4, 5] Defining the efficiency of aircraft was, of course, the usual responsibility of the experimenters.

*At the time of the earlier ground vehicle experiments, the research facility was named NASA Flight Research Center. In May of 1976, the name was changed to the Hugh L. Dryden Flight Research Center, herein referred to as NASA Dryden.

Funds were not available for the rental or purchase of a ground vehicle with which to perform the first drag studies. Consequently, an experimental effort was initiated in 1974 using a modified van that had been retired from hauling mail and making routine deliveries for NASA Dryden (figs. 1(a) and 1(b)).[6] The results of this effort were noticed by the U. S. Department of Transportation (DOT). This agency offered to fund NASA Dryden's entry into 18-wheel heavy-duty truck testing of several "add-on" devices that various manufacturers had been advocating for drag reduction. The DOT reasoned that the coast-down work demonstrated by NASA Dryden[6] represented an objective means of sorting out which add-on devices would be the most effective. NASA Dryden accepted the DOT proposal and consequently had two ground vehicle research facilities, the test van and an 18-wheel cab-over-engine (COE) tractor and semitrailer.

Both vehicles were used in extensive coast-down tests. Subsequently, another tractor and semitrailer of the same make and model were obtained under the DOT arrangement for over-the-highway fuel consumption tests. These tests were concurrent, wherein one vehicle served as the baseline and the other carried a candidate add-on device (fig. 1(c)). Results from follow-on experiments using the test van and the DOT-supported heavy-duty truck tests have previously been published.[7–11*]

The foregoing experiments stimulated follow-on tests that included a major modification to a COE tractor and trailer combination (fig. 1(d)).[12] Coast-down tests were also conducted to evaluate modifications to a two-axle truck, and NASA Dryden sponsored seven separate wind-tunnel model studies of all of the types of vehicle shapes mentioned thus far. The results of this follow-on effort have previously been reported.[12–24] The latest of these references, published in 1983, represented the conclusion of NASA Dryden's active and sponsored participation in ground vehicle aerodynamic research.

During the next decade, truck manufacturers and the interested federal departments (DOT and the Department of Energy) placed increasing attention and effort on improving aerodynamic efficiency of heavy-duty trucks and buses and sponsored joint conferences and workshops. Although NASA Dryden has not been involved in these more recent efforts, representatives were invited to attend and participate in a workshop held in Phoenix, Arizona, January 30–31, 1997.[†] Several of the presentations for the January 30th sessions discussed and proclaimed that a generally accepted goal for drag coefficient of future tractor-semitrailer combinations is 0.25 (van-type trailers). Graphics were provided of recently developed and planned configurations for tractors that are evolving toward achievement of that stated goal. Consideration of the ramifications of these tractor configurations in the context of the stated goal for drag coefficient constitutes the purpose of this publication, as outlined in the discussion section. First, however, a brief overview of attempts to reduce truck drag will be presented as background to the aforementioned drag coefficient goal for future heavy-duty trucks.

BACKGROUND

Minimizing fluid-dynamic drag through careful shaping has been practiced by boat and ship designers for many hundreds of years. Proposals for means to reduce the aerodynamic drag of road vehicles have been made since approximately 1914, when the speed of horsedrawn vehicles began to be exceeded. Because fuel supplies were plentiful and highway speeds were still generally low, serious attempts to

*At the time of these publications (mid 1970's), expected fuel savings, in percent, were understood to be approximately one-half of the percentage reduction in aerodynamic drag.[8, 11]

†The title of the workshop was "U. S. Department of Energy Workshop on Heavy Vehicle Aerodynamic Drag" and was cosponsored by the U. S. Department of Energy and the Lawrence Livermore National Laboratory.

E 26477

(a) Partly constructed test van showing substructure.

E 26574

(b) Test van configuration A (all square corners).

Figure 1. Examples of ground vehicles evaluated at NASA Dryden Flight Research Center.

ECN 4213

(c) Cab-over-engine tractor and semitrailer with cab-mounted add-on device.

ECN 4724

(d) Low-drag cab-over-engine tractor-semitrailer configuration.

Figure 1. Concluded.

reduce aerodynamic drag were sporadic and not often adopted until the oil crisis of the 1970's. This dearth of attention to drag reduction was the norm in the design of heavy-duty trucks despite very credible research performed during the 1950's by the University of Maryland for Trailmobile, Inc. (Chicago, Illinois)[25] and during the 1960's by General Motors Corporation (Detroit, Michigan).[26]

The oil crisis stimulated the development of add-on devices that could be affixed to trucks that were already in use, and workshops such as those represented by reference 8 were organized to disseminate ideas and information. However, the rate of acceptance and use of add-on devices was modest. A private, anecdotal survey was made by this author during the summer of 1975 coincident with a 3600-mile vacation trip (California to Iowa, round trip). This survey, which involved a sample field of 965 tractor-semitrailer vehicles, revealed that 11 percent of the tractor-semitrailer combinations having van-type trailers were using cab-mounted add-on deflector shields. Figure 1(c) shows an air deflector that typifies those devices. More sophisticated cab-mounted devices followed, most for use on COE tractors, which were more numerous than conventional tractors at that time.* These follow-on devices were more "three-dimensional" than the earlier add-ons in that they covered more of the cab roof surface and had substantial volume compared to the earlier panel-type deflectors. Examples of these follow-on devices are the Drag-foiler® developed by GMC Truck and Coach Division (Pontiac, Michigan)[27] and the "streamlined fairing" developed by the University of Maryland.[28]

Although the author does not know when the change began, the conventional, or long-nose, tractor has apparently now replaced the COE tractor as the predominant type. Many of the conventional tractors now carry aerodynamic fairings above and behind the cab that essentially shield the entire front face of the semitrailer from the oncoming airstream. These huge devices also include side panels that reduce the gap length between the tractor fairing and the semitrailer. Figure 2 shows an example of this type of forebody treatment. Although this represents a substantial step toward reducing the tractor and semitrailer forebody drag, the profile view (fig. 2(b)) shows rather severe discontinuities in profile slopes between the top of the engine hood and the above-cab fairing. These discontinuities add to the tractor forebody drag.

Recently (1997–1998), a few tractor models have appeared on the highways that show a significantly smoother profile from the hood region to the above-cab fairing. Figure 3 shows two examples of such configurations, vehicle X and vehicle Y. The sun visors of these tractors are vented at the top, so the effective profiles in this region are relatively smooth irrespective of the silhouetted sun visor images of the profile views. These two tractors typify a trend that will probably continue because their forebodies will do less work on the air and will thereby have low forebody drag, and they tend to shield the front face of the trailer.

Several presentations by representatives of organizations at the aforementioned 1997 Phoenix workshop acknowledged and endorsed the goal of a 0.25 drag coefficient for tractor-semitrailer combinations. These presentations indicated that upcoming tractor configurations would be conventional (long-nose) types with very refined and smooth cross-sectional area development. Conceptual examples shown were reminiscent of futuristic models considered in the 1970's by Servais and Bauer.[8, 29] The conventional tractor style is understood to offer more potential for gradual cross-sectional area development than the COE configuration and perhaps is one reason for the emergence of the conventional type in greater

*The aforementioned 1975 survey also revealed that 79 percent of the tractors sampled were COE and 72 percent of the semitrailers were van-type, as opposed to flat beds or tankers.

EC97 44312-05

(a) Approaching view.

EC97 44312-06

(b) Profile view.

Figure 2. Conventional tractor with fairing that shields trailer front. Forebody profile has significant slope discontinuities.

EC97 44312-01

(a) Vehicle X, approaching view.

EC97 44312-02

(b) Vehicle X, profile view.

Figure 3. Conventional tractors with fairing that shields trailer front. Forebody profile has modest slope changes.

EC97 44312-07

(c) Vehicle Y, approaching view.

EC97 44312-08

(d) Vehicle Y, profile view.

Figure 3. Concluded.

numbers. However, experience at NASA Dryden regarding ground vehicle and flight research and the reported results[6–24] (as well as unpublished results) raise questions and possibilities regarding the relative aerodynamic efficiency of conventional and COE configurations in combination with van-type trailers. These questions and possibilities have arisen in the context of the goal for the coefficient of aerodynamic drag (0.25) for 18-wheel heavy-duty trucks. The consequences of these questions and the development of the possibilities will be discussed in the following section.

DISCUSSION

Truck designers apparently have experimental evidence that a drag coefficient of 0.25 is achievable. In addition, the NASA Dryden ground vehicle experiments conducted from 1974 to 1982 tend to support this possibility. Much of the evidence from NASA Dryden suggesting a drag coefficient of 0.25 as a practical goal derives from the test van experiments. References 6, 7, 10, and 21 chronicle the reduction in drag obtained with this box-shaped vehicle that was achieved through various modifications. The baseline vehicle, configuration A, had square corners at the front and rear and a typical rough or exposed underbody (fig. 1), representing the square-cornered hauler or motor home of the early 1970's. Various modifications were then made, beginning with rounded front corners; and the final configurations had rounded front vertical and horizontal corners, a smoothed underbody, and a boattail (first a full boattail and finally a truncated boattail). The aerodynamic drag reduction achieved by the final configuration (which had the truncated boattail), $C_D = 0.242$, was 73 percent as referenced to the original baseline configuration ($C_D = 0.89$). Figure 4 shows photographs of these two configurations, A and H, and their respective drag coefficients, here based on the conventional reference area. Note how the tuft pattern on the vehicle with square front corners is random, and some tufts, approximately one-third of the way from the front, are swept forward by the large vortex generated by the front corner.

Conversely, configuration H, which had the rounded front corners, exhibits a tuft pattern that indicates attached boundary-layer flow for the entire length of the vehicle, including the boattail. Figure 4(c) shows that attached flow also prevailed over the top surface. This attached flow, the smoothed underbody, and the boattail permit configuration H to have the drag coefficient of 0.242. Figure 5 shows the extent of the attached flow for configurations G and H, which had full and truncated boattails, respectively. Figure 5(a) shows that attached flow prevails over the upper and side boattail surfaces; and even for the lower surface the tufts appear to be aligned streamwise, although gravity is beginning to pull a few tufts away from the surface. The white tufts on the base formed by truncation show the randomness expected in such a thoroughly separated region. The tuft patterns in figure 5(b) and (c) indicate that attached flow extends slightly beyond the truncation line (station) indicated by the sealing tape. This indication is consistent with the only slightly lower drag coefficient for the full boattail as compared to the truncated boattail. Thus, the body station for truncation was well-chosen, albeit somewhat fortuitous in that the choice was based on a combination of flow visualization evidence from the one-tenth scale model tests of reference 13 and a measure of judgment.

Table 1 shows tabulated values of drag coefficients and percentages of drag reduction for each of the eight test van configurations. Table 2 shows highlights of configurational differences for the test van program. For an explanation of the definitions for "NASA Dryden–designated" and "conventional" drag coefficients as represented in table 1, refer to the appendix.

E 26717

(a) Configuration A (baseline). Conventional $C_D = 0.89$.

E 38096

(b) Configuration H. Conventional $C_D = 0.242$.

Figure 4. Comparison of tuft patterns from the baseline configuration and the configuration that has rounded front corners.

E 27062

(c) View showing attached-flow tuft pattern on upper surface when front corners are rounded.

Figure 4. Concluded.

E 38075

(a) Configuration H (truncated boattail). Conventional $C_D = 0.242$.

Figure 5. Tuft patterns for truncated and full boattail configurations.

E 38007

(b) Configuration G (full boattail). Conventional $C_D = 0.238$.

E 38008

(c) Configuration G (full boattail). Conventional $C_D = 0.238$.

Figure 5. Concluded.

Table 1. Test van drag results.

Configuration	C_D, NASA Dryden–designated	$\frac{\Delta C_D}{C_{D_A}}$, percent	C_D, conventional	Reference
A	1.13	0	0.89	6, 7, 10
B	0.68	40	0.54	6, 7, 10
C	0.520	54	0.410	7, 10
D	0.440	61	0.347	7, 10
E	0.443	61	0.350	7, 10
F	0.463	59	0.365	7, 10
G	0.302	73 (.733)	0.238	21
H	0.307	73 (.728)	0.242	21

Table 2. Configuration characteristics.

Configuration*	Corners		Underbody
	Front	Rear	
A	Square	Square	Exposed
B	Vertical rounded, horizontal square	Vertical rounded, horizontal square	Exposed
C	Rounded	Rounded	Exposed
D	Rounded	Rounded	Full-length seal
E	Rounded	Rounded	Three-fourths-length seal
F	Rounded	Square	Three-fourths-length seal
G	Rounded	Full boattail	Full-length seal
H	Rounded	Truncated boattail	Full-length seal

*Configuration F approximates configuration I of reference 21 except that configuration I has a full-length underbody seal (fairing). Configuration G is configuration II and configuration H is configuration III of reference 21. Drag coefficients for configurations G and H are averaged for V = 50 mph and 60 mph. Drag coefficients for configurations A to F were obtained at V = 60 mph.

As indicated in figure 5 and table 1, two of the test van configurations, G and H, achieved conventional drag coefficients slightly below 0.25. In order to obtain this level of drag coefficient, refining the shape of both the front and rear portions of the vehicle was necessary. Smoothing, or enclosing, the underbody so that axles, transmission, fuel tanks, muffler, suspension system and other underbody hardware were shielded from the external air flow was also necessary. Although the results from these two configurations are noteworthy because of their low drag, data from configurations A and F offer insight into an important aerodynamics relationship for the flow over a body having a blunt base. This relationship determines that the more efficient the forebody of a vehicle, the greater the base drag—unless

special effort is applied to reduce afterbody drag.* Both configurations A and F had blunt bases (table 2; figs. 1 and 6), as do present heavy-duty semitrailer van-type haulers. However, configuration A had a very inefficient forebody; and configuration F, which had frontal corner radii that were 20 percent of the vehicle width, had a forebody with very low drag.

E 27719

(a) Viewed at the eleven o'clock position showing rounded front corners.

E 27718

(b) Viewed at the eight o'clock position showing square aft corners.

Figure 6. Configuration F (vehicle at rest); $r/w = 0.2$.

*The text and figures to follow provide help in quantifying the relationship of base drag to forebody drag.

The results from these configurations, considered together, show that special attention to the afterbody design is necessary to achieve the design goal drag coefficient of 0.25. Such efforts may result in greater trailer length that may violate length regulations, especially tractor-semitrailer combinations employing conventional-type tractors with corresponding long wheel bases. The benefits provided by afterbody refinement for van-type trailers encourages reconsideration of shorter wheel base, COE tractors to afford a fraction of overall vehicle length devoted to the modified afterbody. The rationale for this consideration and supporting data from test van configurations A and F and blunt-based free-flight air vehicles follow.

Base pressure measurements were made on the blunt-based test van configurations A and F at a nominal highway speed of approximately 60 mph. Configuration F had an aerodynamically efficient forebody, rounded front corners, and a smoothed underbody.[7, 10] Configuration A had squared front corners and a normal rough underbody; hence, its forebody was very inefficient. These two test van configurations provide an example of how the aerodynamic efficiency (or lack of efficiency) influences the base drag of a ground vehicle.

The base pressure coefficient for configuration F is –0.30[7, 10] and for configuration A is –0.10.* Thus, configuration F, which featured the rounded front corners and efficient attached flow, has three times more base drag than configuration A. This same trend is also evident for the one-tenth scale model results reported in reference 13. This trend is also characteristic of blunt-based aircraft components and missiles, as demonstrated by Hoerner in reference 1. Hoerner assembled data from numerous sources and developed semiempirical expressions that represent the relationship of subsonic base pressure coefficients to the forebody drag of the models under consideration. Hoerner developed a relationship for three-dimensional flow and another for quasi-two-dimensional conditions. These expressions, from reference 1, are as follows:

$$\text{three-dimensional flow: } C_{P_b} = -\frac{0.029}{(C_{D_{f,b}})^{\frac{1}{2}}} \tag{1}$$

$$\text{quasi-two-dimensional conditions: } C_{P_b} = -\frac{0.135}{(C_{D_{f,b}})^{\frac{1}{3}}} \tag{2}$$

Figure 7 shows the base pressure results from both configurations of the test van, full and one-tenth scale, in Hoerner's format along with curves representing the two Hoerner relationships. In addition, another expression for three-dimensional flow is included. This latter curve, from reference 30, is a modification to Hoerner's three-dimensional equation wherein the numerator coefficient of 0.029 is replaced by 0.055. The unflagged symbols in figure 7 represent the base pressure coefficient plotted as a function of forebody drag coefficient, where the forebody drag coefficient is defined as the difference between the total aerodynamic drag coefficient and the base drag coefficient, and the base area of the vehicle is the reference area of the drag coefficient. Thus, by this definition the forebody drag obviously includes aerodynamic losses caused by the wheels and wheel wells in addition to the drag generated by the front face, top, bottom, and side surfaces and protuberances on the vehicle.

*The base pressure data from test van configuration A are previously unpublished. The data were obtained by Robert R. Meyer, Jr. and Glen Horvat in 1982 shortly before NASA Dryden ceased ground vehicle experimentation.

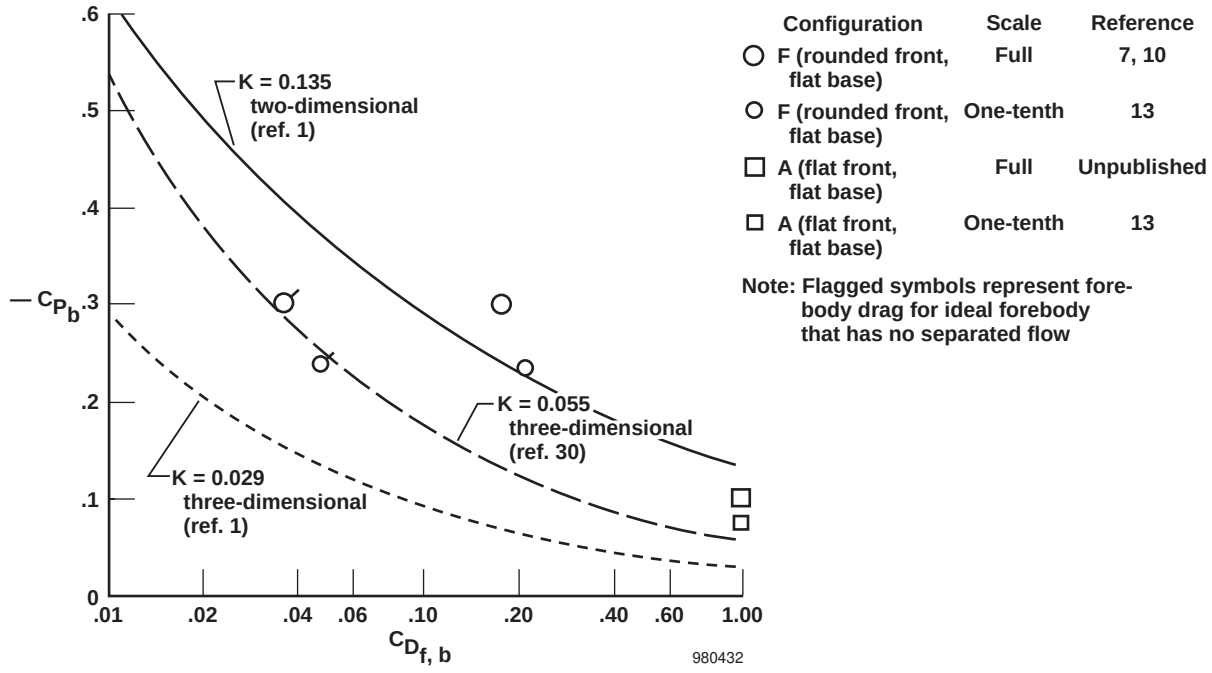

Figure 7. Relationship of base pressure coefficient to forebody drag coefficient for the test van and for two-dimensional and three-dimensional semiempirical equations.

These test van data tend to confirm, in a qualitative way, the trends represented by the three semiempirical expressions from Hoerner. Also included for the test van configurations having rounded front corners are abscissa values for the forebody drag coefficient based on estimated friction losses (the flagged circular symbols). These friction losses are based on an assumed turbulent boundary layer and fully attached flow over all surfaces, top, bottom, and sides, ahead of the base. Thus, the flagged data points represent an ideal body wherein pressure drag from the forward facing front surface, the drag of protuberances, the wheels, and wheel wells are not considered. Thus, a measure of these losses for configuration F is the difference in abscissa position of the flagged and unflagged circular symbols. The ordinate values given the flagged symbols are, of course, the same measured values as for the unflagged data (for example, the base pressure coefficients for the vehicle having wheels and wheel wells).

Although the test van data (full and one-tenth scale) follow the trends of the semiemperical curves of references 1 and 30 in a qualitative way, the degree of similarity is not quantitative. When the semiempirical expressions are assessed against relatively large air vehicles in free flight, the results are as shown in figure 8. The free-flight base pressure data represent results measured on the X-15 research airplane,[31] the X-24B lifting body,[32] and the Space Shuttle shape.[33] In addition, previously unpublished data from the M2-F3 lifting-body are also shown. The forebody drag values for these flight vehicles are obtained from reference 34. Also included are the previously shown results from the test van, configurations A and F (unflagged symbols only).

The free-flight data from the four air vehicles seem to have a closer relationship with Hoerner's quasi-two-dimensional expression than with either of the three-dimensional curves.* This relationship was

*The Δ symbol representing the X-24B lifting body is displaced significantly (C_{P_b} more negative) from the other three air vehicles of comparable forebody drag. This displacement is caused by X-24B longitudinal control surface deflection while the base pressure data were obtained, which, as demonstrated in reference 30, associates configurations that are flared ahead of the base with more negative base pressure coefficients.

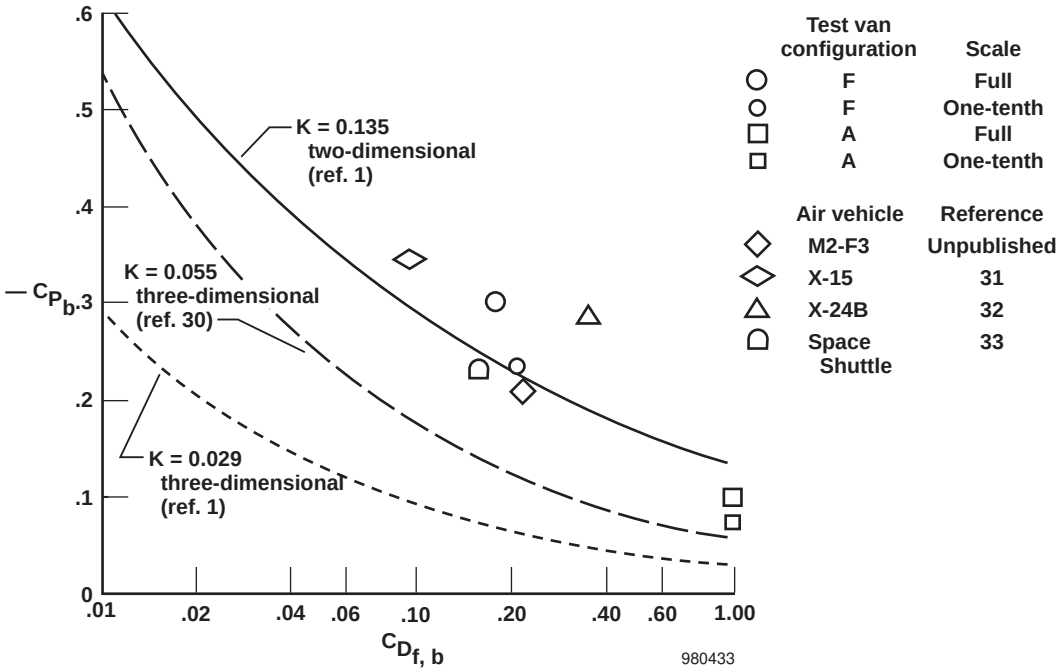

Figure 8. Relationship of base pressure coefficient to forebody drag coefficient for the test van and semiempirical equations and from four air vehicles.

unexpected; however, Hoerner was dependent primarily on small-scale model data when he was developing his equations. His data were mostly from axisymmetric bodies for the three-dimensional shapes, whereas the test van and air vehicle data are asymmetric and of significantly larger scale. The authors of reference 30 were also using small-scale model results when they modified Hoerner's three-dimensional expression, and their models were mostly asymmetric. Although Hoerner's equations produce trends that large-scale results follow, the full-scale results suggest a larger numerator coefficient for the three-dimensional equation for future applications.

Because future large-scale data are obviously not available and all of the vehicles being considered herein are three-dimensional, tentative larger numerator coefficients will be offered here (fig. 9). A shaded region has been added to the relationships already considered. This region represents the Hoerner three-dimensional formula using the numerator coefficient raised to 0.09 for the lower boundary and to 0.10 for the upper boundary. With the exception of the triangular data point representing the X-24B lifting body with the flared afterbody ahead of the base, these coefficients provide a reasonable approximation of the base pressure coefficient–to–forebody drag coefficient relationship formed by the other three air vehicles. At the higher values of forebody drag coefficient, the shaded band approaches the base pressure coefficient level of test van configuration A. A numerator coefficient of 0.12 applied to the Hoerner three-dimensional equation would approximate the base pressure coefficient level for the test van configuration F at full scale.

Figure 10 shows drag coefficient values for a tractor-semitrailer combination for a range of forebody drag coefficients that were calculated using curves representing the relationships shown in figure 9 by the shaded band and the modification of Hoerner's three-dimensional relationship from reference 30. Although the forebody drag coefficients used in Hoerner's equation (and for the abscissa values of

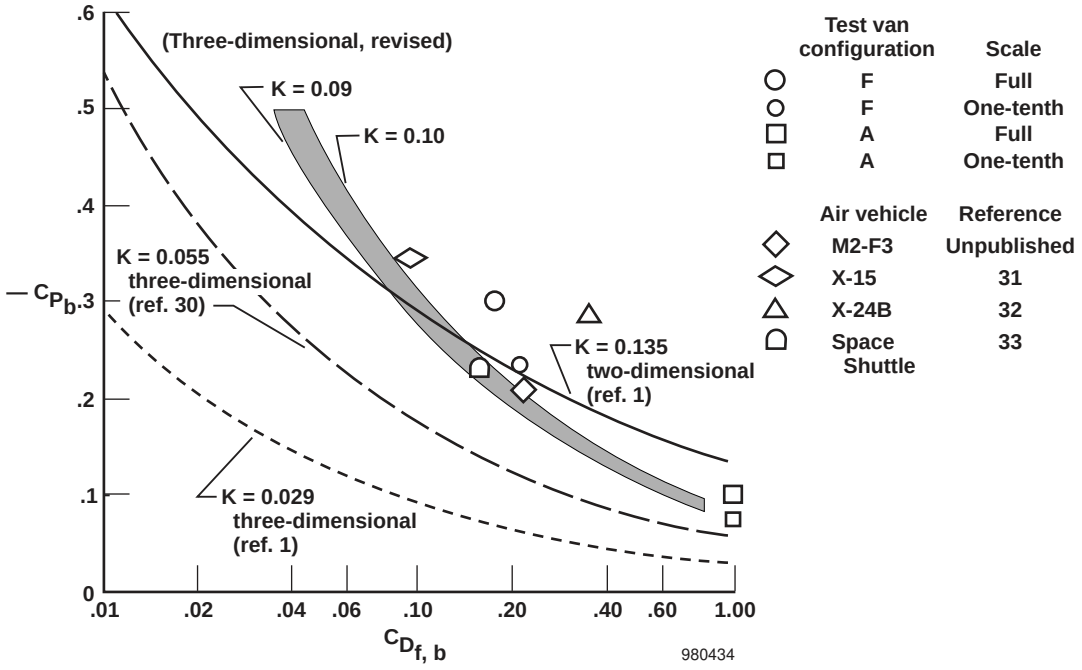

Figure 9. Relationship of base pressure coefficient to forebody drag coefficient for the test van, four air vehicles, and various forms of Hoerner's semiempirical equations.

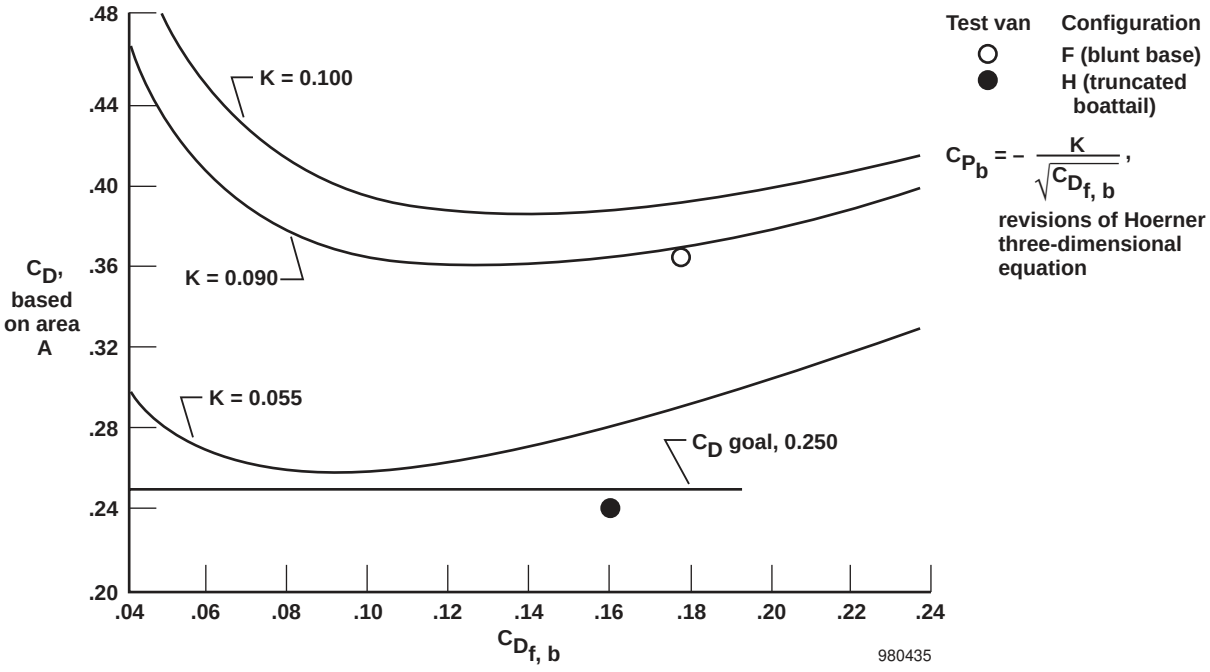

Figure 10. Relationship of total aerodynamic drag coefficient with forebody drag coefficient, based on three versions of Hoerner's three-dimensional semiempirical equations.

figure 10) are referenced to the base area, the ordinate values of total aerodynamic drag coefficient are based upon reference area A as defined in the appendix. This method was used so that the three curves shown in figure 10 could apply directly to the previously mentioned design drag coefficient goal of 0.25. In developing the three curves in figure 10, the tractor-trailer combination is assumed to be smoothly integrated, to have side skirts, and to have a smooth underbody.

Of the three expressions shown in figure 10, only the modification offered by reference 30, K = 0.055, clearly provides a range of conditions over which the C_D goal of 0.25 is approached for a tractor-semitrailer combination having a flat blunt base without afterbody design refinement of some kind. The base pressure data shown in figures 7–9 indicate, however, that the three-dimensional expression having the numerator coefficient of 0.055 does not simulate these large-scale, asymmetric results. Clearly, the pressure coefficient data points shown in figures 7 to 9 are closer to the three-dimensional expressions having the higher numerator coefficients (0.09 to 0.10), which are represented by the two higher curves in figure 10. However, the total drag of a truck having the forebody-to-base drag relationships such as indicated by the two higher drag expressions should also be capable of providing a design goal drag coefficient of 0.25 if proper afterbody refinement is applied. Figures 7–9 show that configuration F at full scale has a base pressure coefficient significantly more negative than all of Hoerner's equations, and revisions thereof, considered thus far. Nevertheless, when a truncated boattail was added (configuration H), a drag coefficient of 0.242 was achieved. Note the data points representing the test van configurations F and H in figure 10.*

Although the various equations developed by Hoerner (and derivations thereof) that are explicit in figures 7 to 9 and implicit in figure 10 may not quantify the best relationship of base drag to forebody drag for large asymmetric vehicles, they are qualitative guidelines of the trends shown by the test van and free-flight vehicles. Therefore, because the modified equation with a numerator coefficient of 0.09 or 0.10 is relatively successful in representing the available large scale data, the relationship employed is considered useful because it facilitates interpretation of these data as follows:

1. Because forebody drag and base drag are additive, and according to the trends illustrated in figure 10, a vehicle having a blunt base without some form of afterbody refinement is unlikely to achieve a drag coefficient of 0.25.
2. Given that afterbody refinement will likely be necessary to achieve this design goal, the curves shown in figure 10 also suggest that the final "definitive" curve will display a modest range of forebody drag coefficient that will result in a minimum overall drag coefficient (a drag "bucket") for that vehicle.†
3. Based on the assumptions operative in the derivation of figure 10 (including the proposed coefficients of 0.09 and 0.10 for Hoerner's three-dimensional equation), minimum achievable drag coefficients range from approximately 0.360 to 0.385 for a blunt-based tractor-trailer combination. The final definition of this minimum drag coefficient will require the accomplishment of the tasks described in items 4 and 5 to follow.

*The area A' is used for reference area of configuration H in figure 10 because A' is the cross-sectional area of the vehicle at the body station where the boattail afterbody begins (rather than using the base area formed by truncation of the boattail). This does not affect the ordinate value of total aerodynamic drag coefficient, 0.242.

†This characteristic is reminiscent of relationships shown in reference 1, pages 6-9, 6-19, 13-2, and 13-6. The concept of such a drag bucket is discussed in greater detail in reference 34.

4. Although actually defining the drag bucket using a highly refined tractor-semitrailer combination would be an interesting challenge for future experimenters, whether a forebody drag coefficient can be achieved low enough to demonstrate the region of minimum drag is uncertain (perhaps unlikely). Nevertheless, the advisability of conducting full-scale coast-down experiments, including base pressure measurements, to work toward defining the drag bucket deserves consideration.

5. Such a tractor-semitrailer combination, or other ground vehicles of comparable fineness ratio, capable of representing a wide range of forebody drag coefficients should be used to define the correct "definitive" base pressure–to–forebody drag relationship. This experiment should be performed even if the complete drag bucket cannot be defined because the test van data used herein may be marginal in scale and is limited to only two values of forebody drag coefficient.

6. If a forebody drag coefficient low enough to define the drag bucket could be achieved, then the least extensive afterbody modifications would be required in order to obtain the design goal of 0.25 for aerodynamic drag coefficient.

The reason for uncertainty as to whether a forebody drag coefficient low enough to define the drag bucket can actually be obtained (item 4 above) is because the apparent target region is approximately 0.10 to 0.16 when forebody drag coefficient is referenced to the base area. Although the forebody drag coefficient of the test van configuration F is close to this region, configuration F had very few protuberances (all small), the underbody was smooth over the forward three-fourths of its length, and the wheel wells were sealed.[7] Configuration H, which had the underbody faired smooth over its entire length, had a somewhat lower forebody drag coefficient. Nevertheless, a significantly lower forebody drag coefficient would be required in order to define the entire drag bucket experimentally. The fact that three of the air vehicles have forebody drag coefficients on the same order as test van configurations F and H reinforces the speculation that, based on data presented thus far, achieving the drag bucket remains uncertain for a vehicle having a conventional blunt base.

The forebody drag coefficients discussed and noted thus far depend on the base area of the respective vehicles as a reference because Hoerner's equation, and derivatives thereof, require base area as a reference. His formulation is very useful toward understanding the various data that are available. Asking whether another logical reference area exists that would either reinforce or dispel the possibility that the test van forebody drag coefficient and some air vehicle forebody losses can be of the same order is reasonable. Because forebody drag is dependent on the flow over the forebody surfaces and any flow separation associated with those surfaces, another logical reference is the total surface area upstream of the base, which is called the "wetted" area.

Figure 11 shows forebody drag coefficients for several subject vehicles using the base area and then the wetted area as a reference. For this comparison, another lifting-body air vehicle, the M2-F1 lifting body, is also included. Figure 11(a) shows the forebody drag coefficients in bar graph form, using the base area as a reference.* In this format, the test van forebody drag coefficients compare favorably with the three lifting-body air vehicles, are of the same order as the Space Shuttle value, and greatly exceed the X-15 forebody drag coefficient. When the wetted area is used as a reference (fig. 11(b)), the test van coefficients are significantly greater than the Space Shuttle and the X-15 vehicle, but of the same order as the remaining air vehicles, which are lifting bodies.

*As noted before, configuration H, in figures 10 and 11(a) uses the same reference area as configuration F—the cross-sectional area of the vehicle where the boattail afterbody begins.

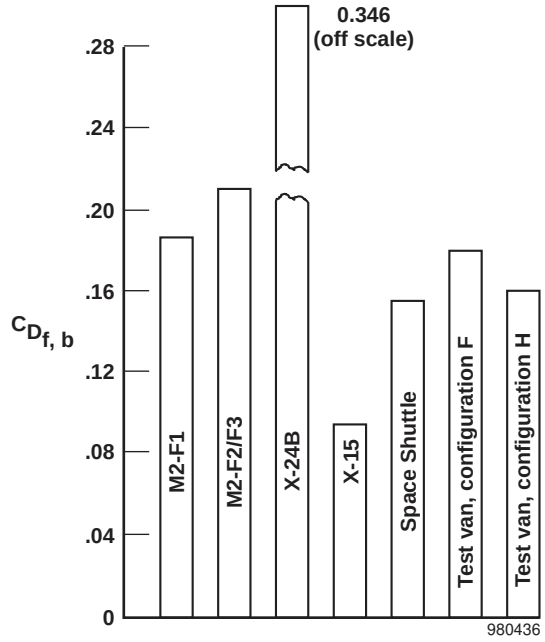

(a) Base area used for reference.

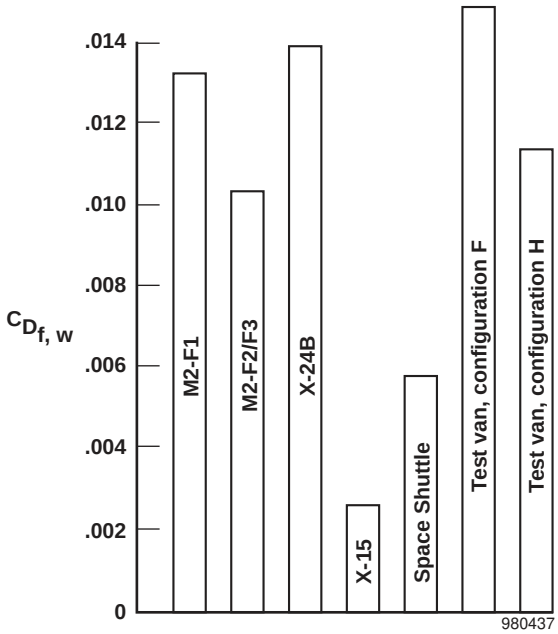

(b) Wetted area used for reference

Figure 11. Influence of reference area choice on comparisons of forebody drag coefficients for several air vehicles and two test van configurations.

Based on figures 11(a) and (b), these test van configurations challenge lifting-body air vehicle shapes for forebody efficiency, and the X-15 and Space Shuttle forebody losses are significantly lower. Because the fineness ratios of the latter two vehicles are higher than most lifting bodies and the test van, fineness ratio is worth examining in greater detail.

Figure 12 shows forebody drag coefficients for several vehicles on the basis of effective fineness ratio, vehicle length divided by effective diameter, where $d_{eff} = \left(\frac{4A_c}{\pi}\right)^{\frac{1}{2}}$ and A_c is the maximum projected forebody cross-sectional area. Although a modest degree of correlation was expected, the degree of order shown in figure 12 was unexpected and is believed to be somewhat fortuitous. Nevertheless, the data show that fineness ratio is a factor that adds order to the apparent large differences in forebody drag coefficient when wetted area is used as a reference.

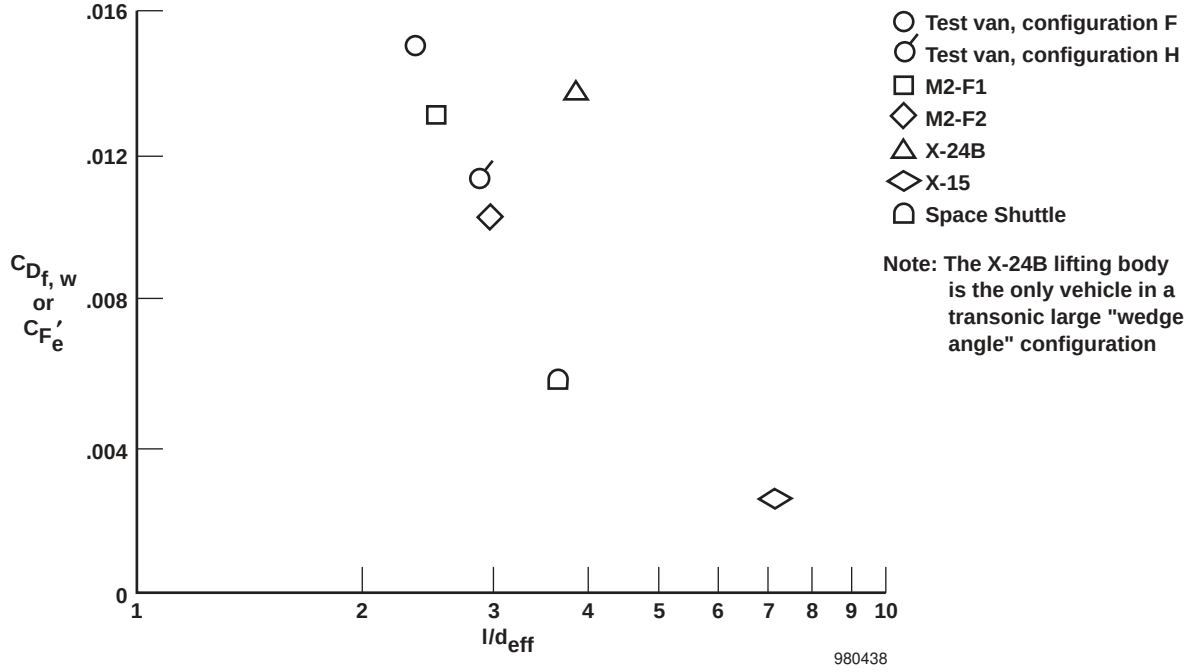

Figure 12. Relationship of forebody drag coefficient with fineness ratio for the subject vehicles.

Excepting the X-24B datum, which is believed to be subject to the large longitudinal control surface "wedge angle" when in the transonic configuration (and possible compressibility effects), the remaining data suggest that:

1. The effect of fineness ratio on the forebody drag coefficient of ground vehicles (in this case, two test van configurations) and air vehicles is similar in nature.
2. Because an advanced integrated tractor-semitrailer combination will have a significantly higher fineness ratio than any of the test van configurations, the potential exists for lower wetted surface forebody losses, as compared to the test van configurations. Such lower losses may afford allowance for a portion of the tire and wheel aerodynamic drag that accompanies an 18-wheel

truck. The effective fineness ratio of an advanced integrated tractor-semitrailer combination is assumed to be at least five (perhaps as much as seven), a factor of two to three greater than for the test van.

Based upon observations made (figs. 10–12), the decision was made to prepare relationships of total drag coefficient with forebody drag coefficient (based upon wetted area) analogous to figure 10. Figure 13 shows the resulting curves, again representing three numerator coefficients for Hoerner's three-dimensional equation. These relationships depend on a specified ratio of wetted area to base area so that the base drag coefficient can be calculated for a given value of forebody drag coefficient based upon wetted area. As with figure 10, the tractor and semitrailer are assumed to be smoothly integrated and have a smooth underbody, side skirts, and a blunt base. The resulting wetted area–to–base area ratio is approximately 23.5, and the effective fineness ratio is 5.25. Assuming that the curves having numerator coefficients of 0.09 or 0.10 for Hoerner's equation are representative of heavy-duty vehicles, wetted area forebody drag coefficient values between approximately 0.004 and 0.008 bracket the bucket region. If a higher value of K is found to better represent heavy-duty vehicles, the bucket region will obviously advance to higher forebody drag coefficients. Based on the relationships shown in figure 12, wetted area forebody drag coefficients between 0.004 and 0.008 are not beyond consideration for effective fineness ratios near 5 (excluding tire, wheel, and wheel-well losses). Thus, careful shielding and fairing of these rolling components must be accomplished in order to limit the forebody drag that would be added to the minimum for attached turbulent flow (shown in figure 13 by the dashed vertical line).*

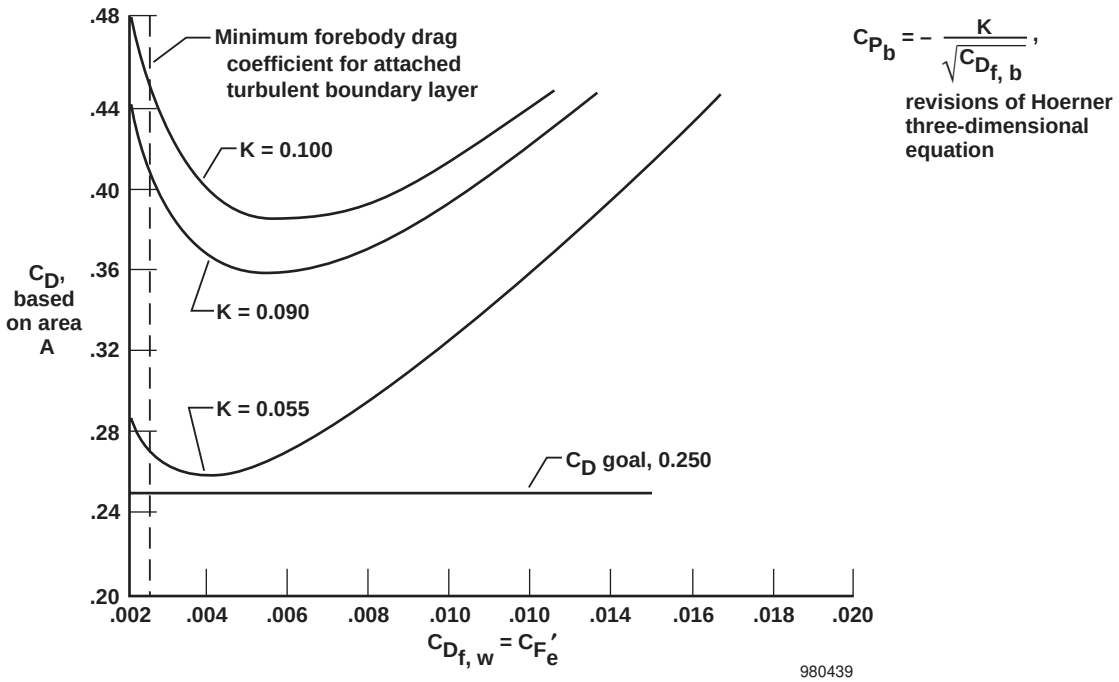

Figure 13. Relationship of total aerodynamic coefficient with forebody drag coefficient (analogous to figure 10) where forebody drag coefficient is based on wetted area.

*The dashed vertical line at 0.0025 on the abscissa represents the forebody drag coefficient, based on the wetted area, that would exist if only friction losses for turbulent flow over a smooth skin forebody existed (no pressure or interference losses).

As figure 10 also shows, these relationships indicate that a large reduction of base drag must occur in order to achieve the drag coefficient goal of 0.25. If the definitive relationship of total aerodynamic drag coefficient to forebody drag coefficient is proven to be reasonably close to the two upper curves of figures 10 and 13, then the test van results included in figure 10 offer encouragement that afterbody refinement may close the gap. The truncated boattail used on the test van is only one approach, but is worthy of consideration in spite of its major departure from contemporary truck design. These lessons learned relative to trucks ought to apply also to long-range, or interstate, buses and motor homes.

Data or information related to vehicle boattail applications can be obtained in references 1, 13, 15–19, 21 and 25, and the patents listed as references 35–37. The concepts offered by these patents are only examples and other more recent patents for boattails are likely to exist, some of which may be more practical. Other means of reducing base drag include castellated or serrated trailing edges,[38, 39] trapped vortices,[40–42] and splitter plates and vented cavities.[1, 43–48] The possibility also exists that base pressure can be increased through application of a moving surface, or rotating cylinder, at the base "turning" station as proposed in references 49 and 50. More information on characteristics of rotating cylinders and the Flettner rotor concept may be obtained in references 51 and 1, respectively. Bearman's careful work and supporting references[52] address several aspects of base drag reduction that deserve consideration. As the titles of some of these references indicate, some of these base refinement data were obtained at moderately high subsonic Mach numbers (0.5 to 0.7). Data obtained within this range have been found to be qualitatively similar to data from very low Mach numbers for trailing edges that produce small radius or sharp corners over which to separate the flow at the base station. Therefore, a base drag reduction device should not be rejected as a candidate for highway speeds solely on the basis of conceptual data having been obtained at moderately high subsonic speeds.

CONCLUDING REMARKS

1. The NASA Dryden Flight Research Center test van, a box-shaped ground vehicle with a truncated boattail afterbody, has achieved an aerodynamic drag coefficient of 0.242. This drag coefficient is slightly lower than the trucking industry and U. S. Department of Energy goal of 0.25.
2. Two versions of the test van ground research vehicle (configurations A and F) demonstrate that as forebody drag is reduced, the base drag is increased. Wind-tunnel tests of these test van shapes at one-tenth scale provide similar trends. Both sets of data, from the research vehicle and the models, verify the trend of the base drag–to–forebody drag relationship formulated by Hoerner.
3. Although the test van ground research vehicle data verify the trend of the Hoerner formulation (qualitative agreement), these data are not in quantitative agreement with the Hoerner equation. For Hoerner's three-dimensional relationship to approach quantitative conformity with the ground research vehicle data (and air vehicle data), the numerator coefficient must be increased by a factor of approximately 3 (a numerator coefficient on the order of 0.09 to 0.10).
4. The relationships described in items 2 and 3 above are also believed to be representative of heavy-duty tractor-semitrailer combinations (van-type trailers). However, in order to quantify such a relationship with certainty for full-scale heavy-duty vehicles, further research is recommended. "Coast-down" tests and base pressure measurements should be performed using a smoothly integrated, full-scale tractor-semitrailer combination or other large vehicle of comparable fineness ratio. The experimental vehicle should have provisions for varying the forebody drag over a range large enough so that a revised numerator coefficient for Hoerner's three-dimensional equation can be defined with certainty (or, if advisable, a superior relationship may be formulated).

5. Because base drag increases as forebody drag is reduced and these components of drag are additive, afterbody refinement (base drag reduction) will be required in order to achieve an overall aerodynamic drag coefficient of 0.25.

6. Assuming that employing afterbody refinement for van-type trailers will be necessary to achieve a design goal drag coefficient of 0.25, designers may want to again use a type of cab-over-engine tractor so that the shorter wheel base can afford extra trailer length devoted to base drag reduction devices.

7. Based on the aforementioned forebody drag and base drag relationships and the consequences mentioned in items 4 and 5 above, tractor and van-type trailer designers are advised to integrate their design efforts and work as a team.

8. Calculations based upon tentative numerator coefficients for Hoerner's three-dimensional equation for base drag demonstrate that in the overall aerodynamic drag–to–forebody drag relationship, a region of minimum drag (over a limited range of forebody drag) exists that will produce the minimum overall drag. A byproduct of the experiments recommended in item 4 above could be the definition of the forebody drag characteristics that will achieve or approach minimum drag for a blunt-based, van-type tractor-semitrailer combination that is smoothly integrated. Accomplishment of this research item would define the least afterbody drag reduction necessary to achieve the design drag coefficient goal of 0.25.

9. The findings and concepts described in this report for heavy-duty trucks are also applicable to long-range buses and motor homes.

Dryden Flight Research Center
National Aeronautics and Space Administration
Edwards, California, September 18, 1998

APPENDIX

The distinction between the "NASA Dryden–designated" drag coefficient and the "conventional" ground vehicle drag coefficient is dependent on the choice of reference area. For example, the respective reference areas can be derived for the test van vehicle used at NASA Dryden Flight Research Center by referring to data shown in figures A-1 and A-2. Using the dimensions shown, $A' = 0.789A$, which accounts for the respective columns of drag coefficient previously shown in table 1 and the differences between the conventional drag coefficients and those published in references 6, 7, 10, and 21.

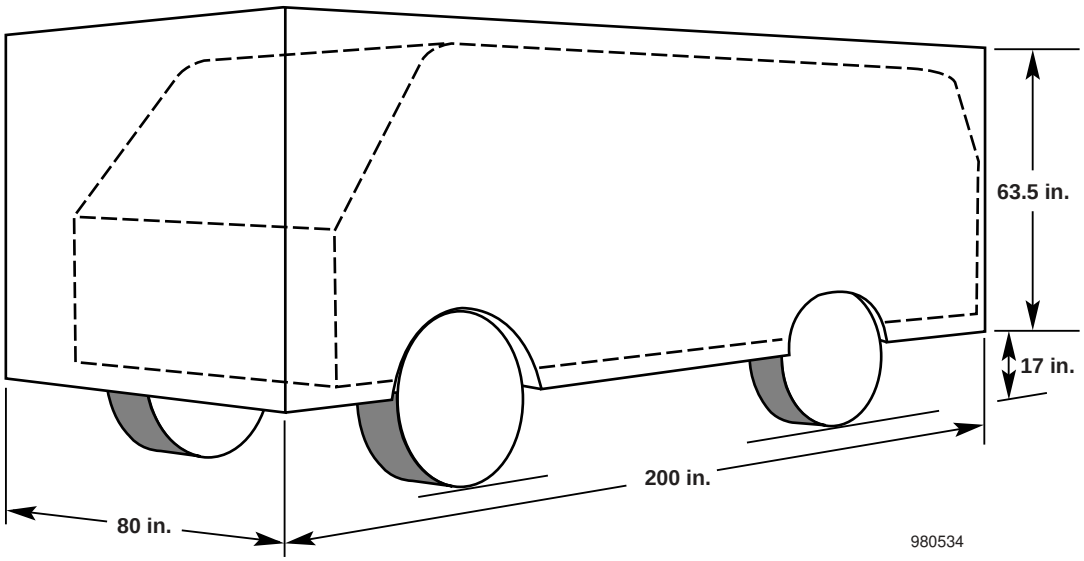

Figure A-1. Test vehicle dimensions for the square-cornered configuration.

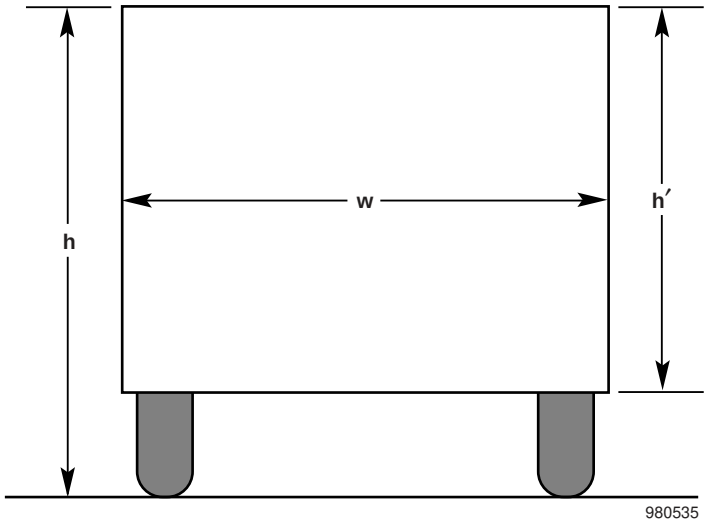

Figure A-2. Sketch to aid understanding of "NASA Dryden–designated" and "conventional" reference areas. A' = NASA Dryden–designated reference area = $w \times h'$. A = conventional reference area = $w \times h$.

The rationale for the NASA Dryden designation has its roots in aeronautical tradition. Aircraft traditionally have their wing planform area assigned as reference area, and dirigibles or blimps are assigned two-thirds power of their volume. These areas are used because they are so closely related to lifting or load carrying capability. Figure A-2 shows that the load carrying capacity of the box-shaped vehicle is more directly related to A' than to A. This rationale led to the NASA Dryden designation of reference area, and hence the higher coefficient for drag. However, because the goal for 18-wheel tractor-semitrailer combinations (van-type) has been defined as an aerodynamic drag coefficient of 0.25 (where the reference area is defined as $w \times h$), the NASA Dryden–designated drag coefficients are herein being transformed by use of the conventional reference area. As table 1 shows, the percentage of reduction of aerodynamic drag for configurations B to H is, of course, unaffected by the definition for reference area that is used.

REFERENCES

1. Hoerner, Sighard F., *Fluid-Dynamic Drag*, Self-published, Midland Park, New Jersey, 1965.

2. White, R. A. and H. H. Korst, "The Determination of Vehicle Drag Contributions from Coast-Down Tests," SAE-720099, Jan. 1972.

3. Roussillon, G., J. Marzin, and J. Bourhis, "Contribution to the Accurate Measurement of Aerodynamic Drag by the Deceleration Method," *Advances in Road Vehicle Aerodynamics 1973*, H. S. Stephens, ed., 1973, pp. 53–62.

4. Keller, Thomas L. and Robert F. Keuper, *Comparison of the Energy Method With the Accelerometer Method of Computing Drag Coefficients From Flight Data*, NACA CB-5H31, 1945.

5. Beeler, De E., Donald R. Bellman, and Edwin J. Saltzman, *Flight Techniques for Determining Airplane Drag at High Mach Numbers*, NACA TN-3821, 1956.

6. Saltzman, Edwin J. and Robert R. Meyer, Jr., *Drag Reduction Obtained by Rounding Vertical Corners on a Box-Shaped Ground Vehicle*, NASA TM-X-56023, 1974.

7. Saltzman, Edwin J., Robert R. Meyer, Jr., and David P. Lux, *Drag Reductions Obtained by Modifying a Box-Shaped Ground Vehicle*, NASA TM-X-56027, 1974.

8. *Reduction of the Aerodynamic Drag of Trucks: Proceedings of the Conference/Workshop,* Oct. 1974, Available from the National Science Foundation, RANN Document Center, 1800 "G" St., N.W., Washington D.C. 20550.

9. Montoya, Lawrence C. and Louis L. Steers, *Aerodynamic Drag Reduction Tests on a Full-Scale Tractor-Trailer Combination With Several Add-On Devices*, NASA TM-X-56028, 1974.

10. Steers, Louis L., Lawrence C. Montoya, and Edwin J. Saltzman, "Aerodynamic Drag Reduction Tests on a Full-Scale Tractor-Trailer Combination and a Representative Box-Shaped Ground Vehicle," SAE -750703, 1975.

11. Steers, L. L. and L. C. Montoya, S*tudy of Aerodynamic Drag Reduction on a Full-Scale Tractor-Trailer*, DOT-TSC-OST-76-13, 1976.

12. Steers, Louis L. and Edwin J. Saltzman, "Reduced Truck Fuel Consumption through Aerodynamic Design," *Journal of Energy*, vol. 1, no. 5, Sept.–Oct. 1977, pp. 312–318.

13. Muirhead, V. U., *An Investigation of Drag Reduction on Box-Shaped Ground Vehicles*, NASA CR-148829, 1976 (also published as KU-FRL #180, University of Kansas).

14. Sheridan, Arthur E. and Steven J. Grier, *Drag Reduction Obtained by Modifying a Standard Truck*, NASA TM-72846, 1978.

15. Muirhead, Vincent U., *An Investigation of Drag Reduction for Tractor Trailer Vehicles*, NASA CR-144877, 1978.

16. Saltzman, Edwin J., "Reductions in Vehicle Fuel Consumption Due to Refinements in Aerodynamic Design," *Institute of Environmental Sciences 1979 Proceedings*, May 1979, pp. 63–68.

17. Muirhead, V. U. and E. J. Saltzman, "Reduction of Aerodynamic Drag and Fuel Consumption for Tractor-Trailer Vehicles," *Journal of Energy*, vol. 3, no. 5, Sept.–Oct. 1979, pp. 279–284.

18. Muirhead, Vincent U., *An Investigation of Drag Reduction for Tractor Trailer Vehicles With Air Deflector and Boattail*, NASA CR-163104, 1981.

19. Muirhead, Vincent U., *An Investigation of Drag Reduction for a Standard Truck With Various Modifications*, NASA CR-163107, 1981.

20. Muirhead, Vincent U., *An Investigation of Drag Reduction for a Box-Shaped Vehicle With Various Modifications*, NASA CR-163111, 1981.

21. Peterson, Randall L., *Drag Reduction Obtained by the Addition of a Boattail to a Box Shaped Vehicle*, NASA CR-163113, 1981.

22. Saltzman, Edwin J., "A Summary of NASA Dryden's Truck Aerodynamic Research," SAE-821284, Nov. 1982.

23. Muirhead, Vincent U., *An Investigation of the Internal and External Aerodynamics of Cattle Trucks*, NASA CR-170400, 1983.

24. Hoffman, J. A. and D. R. Sandlin, *A Preliminary Investigation of the Drag and Ventilation Characteristics of Livestock Haulers*, NASA CR-170408, 1983.

25. Sherwood, A. Wiley, "Wind Tunnel Test of Trailmobile Trailers," University of Maryland Wind Tunnel Report No. 85, June 1953.

26. Flynn, Harold and Peter Kyropoulos, "Truck Aerodynamics," *SAE Transactions 1962*, 1962, pp. 297–308.

27. Kettinger, James N., "Tractor-Trailer Fuel Savings with an Aerodynamic Device—A Comparison of Wind Tunnel and On-Road Tests," SAE-820376, Feb. 1982.

28. Buckley, Frank T., Jr., William H. Walston, Jr., and Colin H. Marks, "Fuel Savings From Truck Aerodynamic Drag Reducers and Correlation With Wind-Tunnel Data," *Journal of Energy*, vol. 2, no. 6, Nov.–Dec. 1978, pp. 321–329.

29. Servais, Ronald A. and Paul T. Bauer, "Aerodynamic Devices Can Significantly Reduce Fuel Consumption of Trucks: Experience with CECA Designs," SAE-750707, Aug. 1975.

30. Butsko, J. E., W. V. Carter, and W. Herman, *Development of Subsonic Base Pressure Prediction Methods*, AFFDL-TR-65-157, vol. 1, Aug. 1965.

31. Saltzman, Edwin J., *Base Pressure Coefficients Obtained From the X-15 Airplane for Mach Numbers up to 6*, NASA TN-D-2420, 1964.

32. U.S. Air Force Flight Vehicle Branch, Aero Mechanics Division, *Correlation of X-24B Flight and Wind Tunnel Pressure Data*, AFFDL-TR-78-93, Sept. 1978.

33. Phillips, W. P, H. R. Compton, and J. T. Findlay, "Base Drag Determination for STS Flights 1-5," AIAA-83-2719, Nov. 1983.

34. Saltzman, Edwin, J., K. Charles Wang, and Kenneth W. Iliff, "Flight Determined Subsonic Lift and Drag Characteristics of Seven Lifting-Body and Wing-Body Reentry Configurations With Truncated Bases," AIAA-99-0393, Jan. 1999.

35. Potter, Ralph B., *Inflatable Streamlining Apparatus for Vehicle Bodies*, United States Patent 2,737,411, Mar. 1956.

36. McDonald, Alan T., *Inflatable Drag Reducer for Land Vehicles*, United States Patent 4,006,932, Feb. 1977.

37. Keedy, Edgar L., *Vehicle Drag Reducer*, United States Patent 4,142,755, Mar. 1979.

38. Tanner, M., "A Method for Reducing the Base Drag of Wings with Blunt Trailing Edge," *Aeronautical Quarterly*, vol. 23, no. 1, Feb. 1972, pp. 15–23.

39. Tanner, M., "Reduction of Base Drag," *Progressive Aerospace Science*, vol. 16. no. 4, 1975, pp. 369–384.

40. Lanser, Wendy R., James C. Ross, and Andrew E. Kauffman, "Aerodynamic Performance of a Drag Reduction Device on a Full-Scale Tractor/Trailer," SAE-912125, Sept. 1991.

41. Powers, Sheryll Goecke, Jarret K. Huffman, and Charles H. Fox, Jr., *Flight and Wind-Tunnel Measurements Showing Base Drag Reduction Provided by a Trailing Disk for High Reynolds Number Turbulent Flow or Subsonic and Transonic Mach Numbers*, NASA TP-2638, 1986.

42. Cornish, Joseph J., III, "Trapped Vortex Flow Control for Automobiles," *Proceedings of the Second AIAA Symposium on Aerodynamics of Sports and Competition Automobiles*, Bernard Pershing, ed., May 1974, pp. 111–118.

43. Nash, J. F., *A Discussion of Two-Dimensional Turbulent Base Flows*, NPL Aero Report 1162, July 1965.

44. Saltzman, Edwin J. and John Hintz, *Flight Evaluation of Splitter-Plate Effectiveness in Reducing Base Drag at Mach Numbers From 0.65 to 0.90*, NASA TM-X-1376, 1967.

45. Powers, Sheryll Goecke, *Influence of Base Modifications on In-Flight Base Drag in the Presence of Jet Exhaust for Mach Numbers from 0.7 to 1.5*, NASA TP-2802, 1988.

46. Pollock, N., *Some Effects of Base Geometry on Two Dimensional Base Drag at Subsonic and Transonic Speeds*, Aerodynamics Note 316, Aeronautical Research Laboratories, Commonwealth of Australia, Oct. 1969.

47. Tanner, Mauri, “New Investigations for Reducing the Base Drag of Wings With a Blunt Trailing Edge,” *Aerodynamic Drag*, AGARD-CP-124, Apr. 1973, pp. 12-1–12-9.

48. Pyle, Jon S. and Edwin J. Saltzman, “Review of Drag Measurements From Flight Tests of Manned Aircraft With Comparisons to Wind-Tunnel Predictions,” *Aerodynamic Drag*, AGARD-CP-124, Apr. 1973, pp. 25-1–25-12.

49. Favre, Alexander, *Aircraft Wing Flap With a Leading Edge Roller*, United States Patent 2,569,983, Oct. 1951.

50. Modi, V., B. Ying, and T. Yokomizo, “Effect of Momentum Injection and Fences on the Drag of a Tractor-Trailer Truck Configuration,” AIAA-92-2640, June 1992.

51. Reid, Elliott G., *Tests of Rotating Cylinders*, NACA TN-209, 1924.

52. Bearman, P. W., “Review—Bluff Body Flows Applicable to Vehicle Aerodynamics,” *Journal of Fluids Engineering*, vol. 102, Sept. 1980, pp. 265–274.

REPORT DOCUMENTATION PAGE

Form Approved
OMB No. 0704-0188

1. AGENCY USE ONLY (Leave blank)	2. REPORT DATE	3. REPORT TYPE AND DATES COVERED
	June 1999	Technical Paper

4. TITLE AND SUBTITLE

A Reassessment of Heavy-Duty Truck Aerodynamic Design Features and Priorities

5. FUNDING NUMBERS

WU 251-10-01-00-TT-00-000

6. AUTHOR(S)

Edwin J. Saltzman and Robert R. Meyer, Jr.

7. PERFORMING ORGANIZATION NAME(S) AND ADDRESS(ES)

NASA Dryden Flight Research Center
P.O. Box 273
Edwards, California 93523-0273

8. PERFORMING ORGANIZATION REPORT NUMBER

H-2283

9. SPONSORING/MONITORING AGENCY NAME(S) AND ADDRESS(ES)

National Aeronautics and Space Administration
Washington, DC 20546-0001

10. SPONSORING/MONITORING AGENCY REPORT NUMBER

NASA/TP-1999-206574

11. SUPPLEMENTARY NOTES

Edwin J. Saltzman, Analytical Services & Materials, Edwards, California; Robert R. Meyer, Jr., Dryden Flight Research Center, Edwards, California.

12a. DISTRIBUTION/AVAILABILITY STATEMENT

Unclassified—Unlimited
Subject Category 02, 31, 37, 85, 99

12b. DISTRIBUTION CODE

13. ABSTRACT (Maximum 200 words)

Between 1973 and 1982, the NASA Dryden Flight Research Center conducted "coast-down" tests demonstrating means for reducing the drag of trucks, buses, and motor homes. Numerous configurations were evaluated using a box-shaped test van, a two-axle truck, and a tractor-semitrailer combination. Results from three configurations of the test van are of interest now in view of a trucking industry goal of a 0.25 drag coefficient for tractor-semitrailer combinations. Two test van configurations with blunt-base geometry, similar to present day trucks (one configuration has square front corners and the other has rounded front corners), quantify the base drag increase associated with reduced forebody drag. Hoerner's equations predict this trend; however, test van results, reinforced by large-scale air vehicle data, indicate that Hoerner's formula greatly underestimates this dependence of base drag on forebody efficiency. The demonstrated increase in base drag associated with forebody refinement indicates that the goal of a 0.25 drag coefficient will not be achieved without also reducing afterbody drag. A third configuration of the test van had a truncated boattail to reduce afterbody drag and achieved a drag coefficient of 0.242. These results are included here and references are identified for other means of reducing afterbody drag.

14. SUBJECT TERMS

Aerodynamics, Buses, Drag, Ground vehicles, Motor homes, Trucks

15. NUMBER OF PAGES

38

16. PRICE CODE

A03

17. SECURITY CLASSIFICATION OF REPORT	18. SECURITY CLASSIFICATION OF THIS PAGE	19. SECURITY CLASSIFICATION OF ABSTRACT	20. LIMITATION OF ABSTRACT
Unclassified	Unclassified	Unclassified	Unlimited